Experimental Cell Research 345 (2016) 17–24

Contents lists available at ScienceDirect

Experimental Cell Research

journal homepage: www.elsevier.com/locate/yexcr

Research article

Fibroblast spheroids as a model to study sustained fibroblast quiescence and their crosstalk with tumor cells

Pertteli Salmenperä [a,*,1], Piia-Riitta Karhemo [b,1], Kati Räsänen [a], Pirjo Laakkonen [b,1], Antti Vaheri [a,1]

[a] Department of Virology, Medicum, Faculty of Medicine, University of Helsinki, P.O. Box 21, FIN-00014, Finland
[b] Research Programs Unit, Translational Cancer Biology, and Institute of Biomedicine, University of Helsinki, P.O. Box 63, FIN-00014, Finland

ARTICLE INFO

Article history:
Received 28 September 2015
Received in revised form
6 May 2016
Accepted 8 May 2016
Available online 10 May 2016

Keywords:
Fibroblast activation
Nemosis
Secretory phenotype
Cellular senescence, quiescence

ABSTRACT

Stromal fibroblasts have an important role in regulating tumor progression. Normal and quiescent fibroblasts have been shown to restrict and control cancer cell growth, while cancer-associated, i. e. activated fibroblasts have been shown to enhance proliferation and metastasis of cancer cells. In this study we describe generation of quiescent fibroblasts in multicellular spheroids and their effects on squamous cell carcinoma (SCC) growth in soft-agarose and xenograft models. Quiescent phenotype of fibroblasts was determined by global down-regulation of expression of genes related to cell cycle and increased expression of p27. Interestingly, microarray analysis showed that fibroblast quiescence was associated with similar secretory phenotype as seen in senescence and they expressed senescence-associated-β-galactosidase. Quiescent fibroblasts spheroids also restricted the growth of RT3 SCC cells both in soft-agarose and xenograft models unlike proliferating fibroblasts. Restricted tumor growth was associated with marginally increased tumor cell senescence and cellular differentiation, showed with senescence-associated-β-galactosidase and cytokeratin 7 staining. Our results show that the fibroblasts spheroids can be used as a model to study cellular quiescence and their effects on cancer cell progression.
© 2016 Elsevier Inc. All rights reserved.

1. Introduction

In healthy tissue, fibroblasts are maintained in an inactive state and they regulate the proper tissue architecture by controlling the composition of extracellular matrix (ECM). During wound healing and in pathological conditions, such as inflammation and cancer, they become activated and begin to secrete cytokines and growth factors [1,2]. In cancer, these activated fibroblasts (cancer-associated fibroblasts, CAFs) can support cancer progression [1,2], whereas normal fibroblasts have been shown to restrict cancer growth [2,3]. A better understanding of the transition of fibroblasts from quiescence into active state would aid the understanding of cancer progression. Cellular quiescence is not merely a passive arrest in response to nutrient starvation, loss of adhesion or acquisition of confluence, but it seems to be a controlled program with active metabolism and where reversibility is ensured and terminal differentiation is suppressed [4,5].

Nemosis is an experimental model of fibroblast remodeling caused by detaching fibroblasts from their growth support and allowing them spontaneously form multicellular spheroids (reviewed in ref [6]). Nemosis was initially characterized by induction of the stress protein cyclooxygenase-2 (COX-2) [7], an important mediator of inflammation and carcinogenesis [8]. During nemosis the gene expression profile of fibroblasts is altered and they up-regulate expression of cytokines (interleukin (IL)− 1β, IL-6, IL-8, IL-11, granulocyte-macrophage colony-stimulating factor (GM-CSF), leukemia inhibitory factor (LIF), chemokines (MIP-1α, RANTES), growth factors (hepatocyte growth factor (HGF), vascular endothelial growth factor (VEGF), keratinocyte growth factor (KGF)) and proteases (matrix metalloproteinase (MMP)-1, MMP-10, MMP-14, and plasminogen activation [9–14]. Furthermore, nemotic fibroblasts induce migration of melanoma cells [10] and keratinocytes [15], whereas in leukemia cells they cause proliferation arrest and induce differentiation of c-Met-negative cells to dendritic-like cells *in vitro* [12]. However, the effect of nemotic fibroblasts on tumor growth has not been studied *in vivo*.

In this study, we analyzed phenotype and gene expression profile of fibroblast spheroids and analyzed their effect on the growth of metastatic variant of human keratinocyte-derived HaCaT cell line (RT3) [16] both *in vitro* and in xenograft tumors *in vivo*. We show that fibroblast spheroids enter quiescence and that these quiescent fibroblasts are able to slower tumor growth when tumors are formed in their presence. We also show that fibroblasts spheroids provide a useful model to study sustained quiescence and its cross-talk with cancer cells.

* Corresponding author.
E-mail address: pertteli.salmenpera@helsinki.fi (P. Salmenperä).
[1] These authors contributed equally.

http://dx.doi.org/10.1016/j.yexcr.2016.05.005
0014-4827/© 2016 Elsevier Inc. All rights reserved.

2. Materials and methods

2.1. Cell cultures

Human foreskin dermal fibroblasts (HFSF) (kindly provided by Dr. Magdalena Eisinger, Memorial Sloan-Kettering Cancer Center, New York), HT-1080 (American Type Cell Culture Collection, Manassas, VA), AT9733 (American Type Cell Culture Collection) and RT3 (kindly provided by Prof. Dr. Petra Boukamp and Prof. Dr. Norbert E. Fusenig, DKFZ, Heidelberg, Germany) cells were cultured in DMEM/F-12 or DMEM medium (Invitrogen, Carlsbad, CA) supplemented with 5% FCS (Invitrogen), 100 μg/ml streptomycin, and 100 U/ml penicillin. Fibroblast spheroid formation was initiated as previously described [7]. In brief, 200 μl aliquots/well of single cell suspensions (5×10^4 cells/ml; 10,000 cell per well) were plated on agarose-pretreated U-bottom 96-well plates (Costar, Cambridge, MA). Only one spheroid was formed per well.

2.2. Soft-agar assay

The soft-agar colony forming assays were performed as previously described [9]. Briefly, for monolayer group fibroblast were seed normally to cell 6-well cell culture plate and allowed to form monolayer over night. On a following morning monolayer was overlayed with 0.5% agarose diluted in growth medium and let to solidify. For spheroid group fibroblast spheroids were mixed in 0.5% agarose diluted in growth medium that was poured to 6-well cell culture plate and let to solidify. Five thousand RT3 cells/well were mixed to 0.3% agarose diluted in growth medium and laid on the top of bottom agarose. Plates were put to cell incubator for 25 days and formed RT3 colonies were photographed and images were analyzed using NIH ImageJ software (http://rsb. info. nih. gov/ij/).

2.3. Immunofluorescence and senescence-associated β-galactosidase staining

Spheroids were collected at the indicated times and embedded in Tissue Tek OCT (Sakura Finetek, Tokyo, Japan) or paraffin. Immunohistochemistry was performed using the Ventana Discovery immunohistochemistry Slide Stainer (Ventana Medical Systems, Tuscon, AZ). Senescence-associated-β-galactosidase (SA-β-gal) activity was detected as described [17]. The results were interpreted by three experienced users.

2.4. Immunoblotting

Samples were run in 8–20% gradient SDS-PAGE, transferred to nitrocellulose membranes, and incubated with indicated antibodies. Immunoreactive proteins were visualized with the appropriate primary and secondary antibodies using ECL detection (Pierce, Rockford, IL). Densitometric analysis of autoradiographs was performed using the NIH ImageJ software.

2.5. FACS

Cell were fixed with 70% ethanol, washed and stained with propidium iodide (10 μg/ml) (Invitrogen) and analyzed with FACScanner (BD Biosciences, San Jose, CA).

2.6. RNA isolation and microarray analysis

RNA for the microarray analysis was extracted using Trizol Reagent (Invitrogen) and purified with the RNeasy kit (QIAGEN). HG-U133A GeneChips (Affymetrix, Santa Clara, CA) were processed according to manufacture's instructions. Data were analyzed with Affymetrix® Microarray Suite 5.0 and GeneSpring™ software (Agilent Technologies, Palo Alto, CA).

2.7. Xenograft model

In order to generate tumors, RT3 cells alone, with fibroblasts or with fibroblast spheroids were mixed with growth factor reduced Matrigel (BD Biosciences), and injected subcutaneously in the abdominal area of Balb/c nude (Scanbur, Sweden) or NOD/SCID (Charles Rivers Laboratories International, Wilmington, MA) mice. Tumor growth was monitored by measuring the volume using a manual caliber. All animal experiments were performed according to the guidelines approved by the ethics committee of the National Laboratory Animal Center Finland (License number STU 237 A/ESLH-2006-00185/Ym-23, Kuopio, Finland).

3. Results

3.1. Nemotic fibroblasts suppress the growth of human keratinocyte-derived RT3 cells

We have previously shown that the nemotic fibroblasts enhance migration of RT3 cells, a metastatic variant of the human keratinocyte-derived HaCaT cell line [16], through soluble mediators [14]. Therefore, we investigated the effect of nemotic fibroblasts on the growth of RT3 cells in more detail by using a soft-agar assay. Cells were seeded in the top agar and different amounts of fibroblast spheroids (96 or 180, each spheroid contained approximately 10,000 cells) were placed in the bottom layer. As a control, we plated different amounts (0, 50,000, 500,000) of fibroblasts grown as monolayer under the bottom agar. During the experiment (25 days) monolayer control cells grew until they reached confluency (approximately 800,000 cells/well). Fibroblast monolayer supported the growth of RT3 cell colonies and resulted significantly larger colonies. Small number of fibroblast spheroids (96) similarly enhanced the growth of RT3 cell colonies, whereas higher number of the fibroblast spheroids (180) reversed the enhancement effect and resulted colonies similar in size as the RT3 cell colonies growth without fibroblasts (Fig. 1(A)). Fibroblast spheroids also changed the shape of RT3 colonies from round to irregular while the RT3 colonies grown on top of the monolayer fibroblasts or without fibroblasts (control group) remained round. These irregular colonies also appeared to be decomposed (Fig. 1(B)).

To address the effect of quiescent fibroblasts on tumor growth *in vivo*, we implanted RT3 cells alone, with the monolayer-cultured fibroblasts or with fibroblast spheroids into subcutaneously immunocompromised nude mice. We monitored the tumor growth by measuring the tumor volume twice a week for 34 days. Similar to the soft-agar assay, fibroblast spheroids inhibited the growth of RT3 tumors compared to tumors derived from RT3 cells alone or RT3 cells grown with the monolayer fibroblasts. Both the tumor volume and tumor weight were significantly smaller in the fibroblast spheroid group at the end of the experiment (day 34) (Fig. 1(C) and (D)). Similar results were obtained using the NOD/SCID mouse strain (Supplementary figs. S1A and S1B).

3.2. Nemotic fibroblasts enter quiescence

To better understand the tumor growth suppressive function of nemotic fibroblasts we characterized their expression profile using Affymetrix microarrays at 3, 12, 24 and 36 h after initiation of spheroid formation and compared it to that of monolayer fibroblasts. An extensive change in the gene expression pattern, both in number and in fold induction, was seen in the fibroblast spheroids

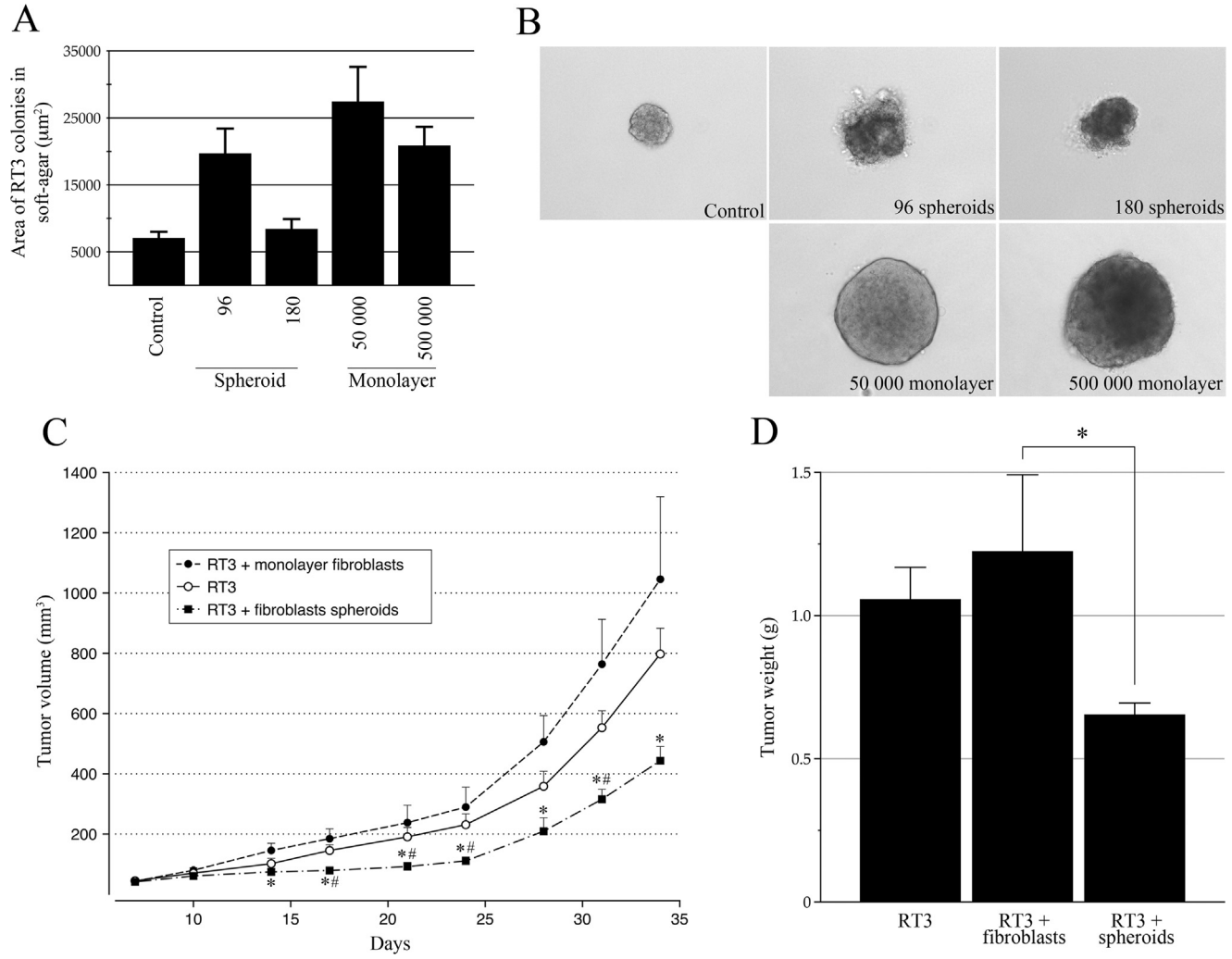

Fig. 1. Effect of fibroblast spheroids on malignant RT3 cells in the soft-agar assay and RT3 tumor growth in nude mice. Indicated amounts of fibroblasts spheroids were plated in bottom agarose and RT3 cells in the top agarose. As a control, indicated amounts of monolayer fibroblasts were grown under the bottom agarose. Experiment was performed in duplicate and three images were taken per well and quantified. (A) Quantification of RT3 colonies formed after 25 days. (B) Morphology of RT3 colonies at day 25. (C) Growth curves of RT3, RT3+ monolayer fibroblasts or RT3+ fibroblast spheroid-containing tumors in nude mice at indicated days. RT3 cells (600,000) were injected subcutaneously alone, or with 360,000 fibroblasts or with 36 spheroids in the abdominal area of the animals. Each group contained six animals; two animals of each group were sacrificed after 10 days and four animal after 34 days. Tumor volume was measures every second day using a caliber. Values represent means+SEM. *=$p<0.05$ (compared to RT3+ fibroblast group) #=$p<0.05$ (compared to RT3 group). (D) Weight of tumors at day 34. At the end of the experiment animals were sacrificed and tumors were excised and weighted. Values represent means +SEM. *= $p<0.05$.

Table 1
Change in the gene expression profile of fibroblast spheroids compared to that of monolayer fibroblasts led to a secretory phenotype, arrest in cell cycle and down-regulation of cytoskeletal proteins. Up-regulated genes were mostly secreted molecules, whereas down-regulated genes were associated with cell cycle or cytoskeleton in fibroblast spheroids compared to monolayer fibroblasts.

Gene Ontology Slims annotation of 2-fold up- and downregulated gene lists at 36 h					
Upregulated			Downregulated		
Gene Ontology	List name	p value	Gene Ontology	List name	p value
Biological process	Cell death (GO:0008219)	8.41×10^{-8}	Biological process	Cytoskeleton organization and biogenesis (GO:0007010)	8.01×10^{-19}
Biological process	Cell-cell signaling (GO:0007267)	2.35×10^{-7}	Biological process	Cell cycle (GO:0007049)	1.86×10^{-9}
Biological process	Cell proliferation (GO:0008283)	0.0239	Cellular component	Cytoskeleton (GO:0005856)	1.46×10^{-13}
Cellular component	Extracellular space (GO:0005615)	0.0334	Cellular component	Microtubule organizing center (GO:0005815)	3.7×10^{-8}
Molecular function	Apoptosis regulator activity (GO:0016329)	1.1×10^{-7}	Molecular function	Actin binding (GO:0003779)	0.011
			Molecular function	Nucleotide binding (GO:0000166)	0.000185
			Molecular function	Motor activity (GO:0003774)	2.11×10^{-11}
			Molecular function	Structural molecule activity (GO:0005198)	4.64×10^{-7}

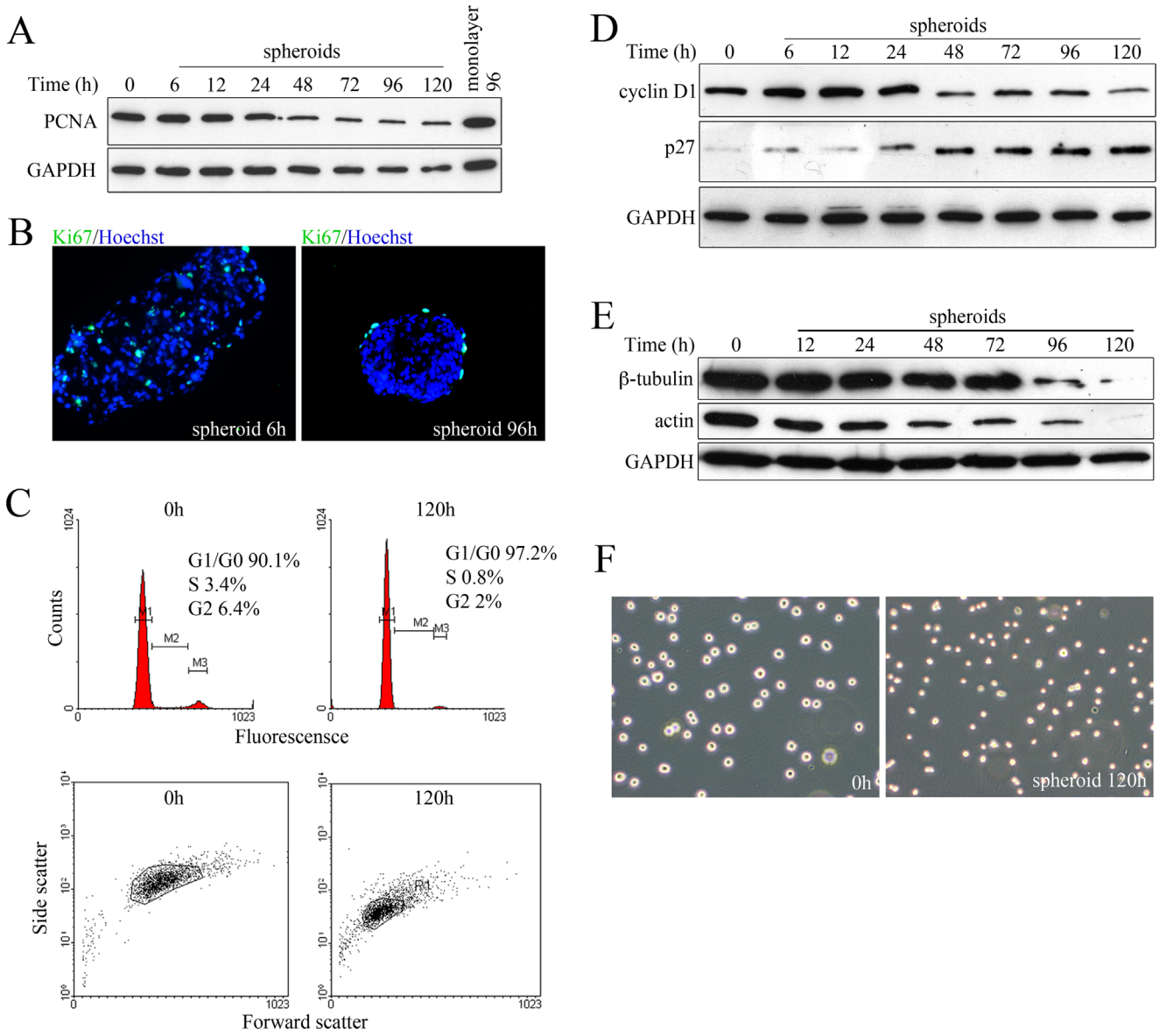

Fig. 2. Nemosis-induced cell cycle arrest of fibroblasts. (A) Down-regulation of PCNA in fibroblast spheroids. Spheroids were lysed at 0, 6, 12, 24, 48, 72, 96 and 120 h after initiation of the spheroid culture, and the extracts were analyzed for the presence of PCNA by immunoblotting. Extracts of the monolayer culture at 96 h were used as a control. Cells in fibroblast monolayers proliferated during the whole experiment. GAPDH was used as a loading control. (B) Down-regulation of cell proliferation in spheroid cultures. Spheroids were stained with an antibody against the Ki67 (a proliferation marker; green) at 0 and 96 h after initiation of the spheroid culture. Ki67-positive cells remained only at the outermost layer of spheroid at 96 h. Hoechst staining (blue) was used to visualize nuclei. (C) Cell cycle was arrested in the fibroblast spheroids. FACS analysis of cell DNA content of spheroid fibroblasts shows accumulation of cells in the G1/G0 at 120 h (G1/G0: 97.2%, S: 0.8%, G2: 2%) compared to 0 h time point (G1/G0: 90.1%, S: 3.4%, G2: 6.4%). M1 = G1/G0 phase, M2 = S phase and M3 = G2 phase. Cell population also shifted towards origo on the forward scatter –axis at 120 h compared to the 0 h time point indicating reduction in cell size. (D) Down-regulation of cell cycle protein cyclin D1 and up-regulation of cell cycle inhibitor p27 in the fibroblast spheroids. Spheroids were lysed at 0, 6, 12, 24, 48, 72, 96 and 120 h after initiation of the spheroid culture and the extracts were analyzed for the presence of cyclin D1 and p27 by immunoblotting. GAPDH was used as a loading control. (E) Down-regulation of cytoskeletal proteins β-tubulin and actin in the fibroblast spheroids. Spheroids were lysed at 0, 12, 24, 48, 72, 96 and 120 h after initiation of the spheroid culture, and the extracts were analyzed for the presence of β-tubulin and actin by immunoblotting. GAPDH was used as a loading control. (F) Cells in fibroblast spheroids were smaller than the cells grown as monolayer culture. Phase-contrast micrographs of cells detached at 0 h and 120 h after initiation of the fibroblast spheroid culture.

compared to the monolayer culture (Supplementary Table S1, Supplementary figs. S2A and S2B). When we compared the lists of up- and down-regulated transcripts to the Gene Ontology Slims gene lists, the down-regulated genes were mostly associated with the cytoskeleton, organelle and cytoplasm organization as well as with the cell cycle (Table 1 and Supplementary Table S1).

To validate the expression microarray results we characterized further the cells in the spheroids. Cell number analyses revealed decreased number of cells in fibroblast spheroids over 96 h experiment. Cell number in spheroids decreased approximately to half over 120 h experiment (12 h: 49,200 cells/ml, 24 h: 46,800 cells/ml, 48 h: 37,200 cells/ml, 72 h: 32,400, 96 h: 28,800 cells/ml and 120 h: 24,000 cells/ml), whereas in monolayer culture fibroblasts expanded exponentially (12 h: 31,500 cells/ml, 24 h 30,000 cells/ml, 48 h 75,600 cells/ml, 72 h 108,000 cells/ml, 96 h: 79,200 cells/ml and 120 h: 73,200 cells/ml) (Supplementary Fig. S2C). The number of proliferating cells as judged by the proliferating nuclear antigen (PCNA) and Ki67 analyses using immunoblotting and immunofluorescence (Fig. 2(A) and (B)) confirmed decreased proliferation of nemotic fibroblasts. Fluorescence-activated cell sorting (FACS) analysis of DNA content revealed that cell cycle was arrested in the G1/G0 phase in the nemotic fibroblast spheroids

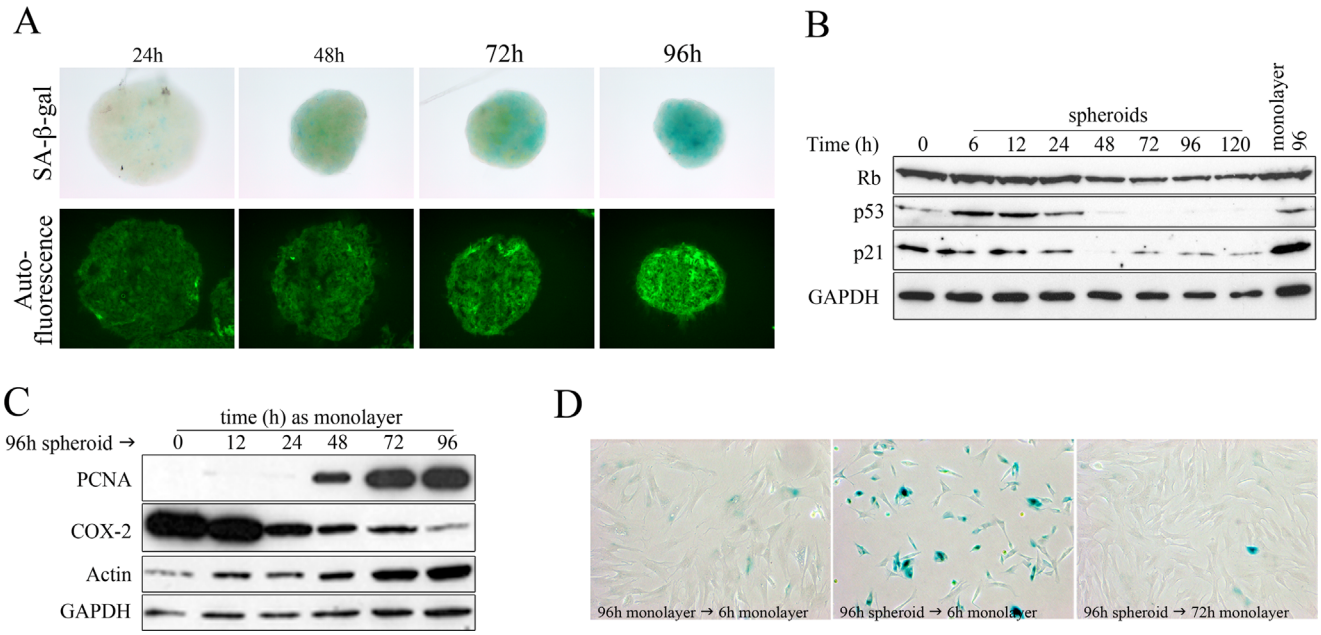

Fig. 3. Regulation of markers of cellular senescence in the fibroblast spheroids. (A) Induction of known markers of senescence. SA-β-gal staining and autofluorescence of fibroblast spheroids at 24, 48, 72 and 96 h. (B) Down-regulation of classical pathways that mediate senescence Rb, p53, p21 at 0, 6, 12, 24, 48, 72, 96 and 120 h in fibroblast spheroids analyzed by immunoblotting. Monolayer fibroblasts at 96 h were used as control to show the continuous proliferation of adherent fibroblasts. GAPDH was used as a loading control. (C) Immunoblot analysis of COX-2, PCNA and actin expression in monolayer fibroblasts (at 0, 12, 24, 48, 72 and 96 h) that were first grown as spheroids for 96 h followed by transfer to a monolayer culture for indicated times. GAPDH was used as a loading control. (D) Reversibility of SA-β-gal staining. Fibroblasts were negative for the SA-β-gal staining when grown in monolayer culture but became positive when kept in spheroid culture for 96 h detached from the spheroids and incubated for 6 h in standard 2D-culture conditions. SA-β-gal staining disappeared when cells were incubated for additional 72 h in the standard 2D culture.

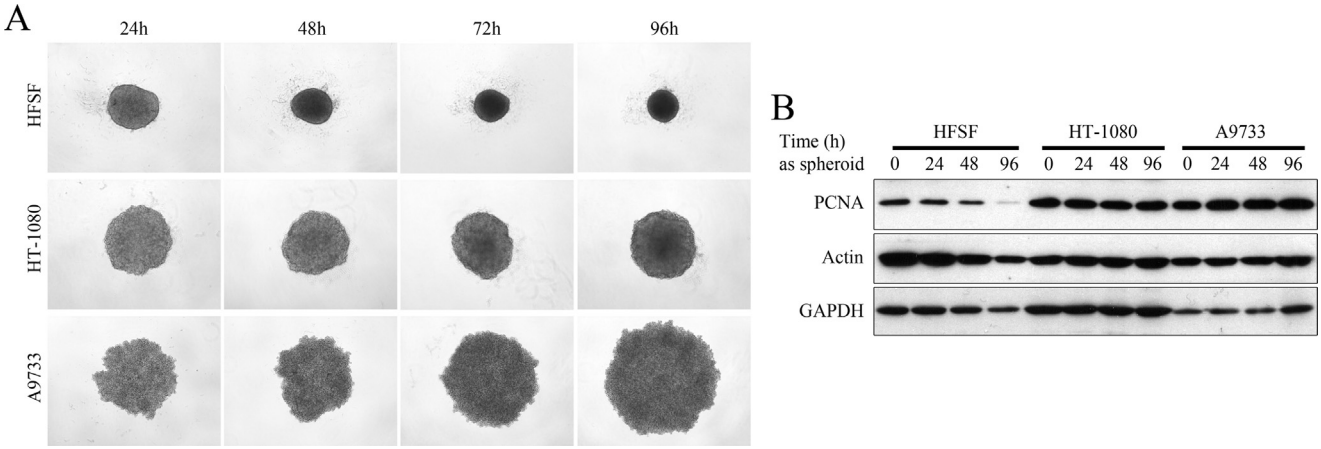

Fig. 4. Fibrosarcoma cell lines are resistant to nemosis. (A) Morphological images of normal human fibroblasts (HFSF) and human fibrosarcoma cells (HT-1080 and A9733) grown under spheroid culture conditions for different time points (24, 48, 72 and 96 h). (B) Immunoblot analysis of PCNA and actin in normal human fibroblasts (HFSF) and human fibrosarcoma cells (HT-1080 and A9733) grown under spheroid culture conditions for different time points (24, 48, 72 and 96 h). GAPDH was used as a loading control.

(Fig. 2(C)). At 120 h the majority (97.2%) of cells in spheroids were in the G1/G0 phase (S 0.8% and G2 2%), whereas at 0 h 90.1% cells were at G1/G0 phase (S 3.4% and G2 6.4%). Accumulation of the G1/G0 phase cells started already at 12 h (Supplementary Figure S2D). The cell cycle arrest at G1/G0 was most likely mediated by the observed 65.8-, 132.3-, 33.8- and 8.9-fold down-regulation of expressions of cyclins A2, B1, B2 and E2, respectively, in the fibroblast spheroids. We also detected down-regulation of cyclin D1, which is crucial for the transition from G1 [18], and up-regulation of p27 protein, a cyclin D1 inhibitor, at the protein level in the spheroids (Fig. 2(D)).

Down-regulation of cytoskeleton-associated genes (Table 1) was confirmed by measuring actin and β-tubulin protein levels by immunoblot analyses (Fig. 2(E)). This down-regulation resulted in substantial decrease in size of cells in fibroblast spheroids as seen by a shift of cell population closer to origo at the forward scatter – axis (Fig. 2(C) and Supplementary Fig. S2D) in the FACS analysis. The change in cell size was visible already at 24 h after initiation of spheroid formation (Supplementary Fig. S2D), and could also be detected using the phase-contrast microscopy (Fig. 2(F)).

Genes of up-regulated mRNAs were confined to biological processes associated with cell death, cell-cell signaling and cell proliferation (Table 1 and Supplementary Table S1). Interestingly, most of the up-regulated mRNAs in fibroblast spheroids produced secreted proteins (cytokines, chemokines and growth factors) such as IL-1α, IL-1β, IL-1RA IL-6, IL-8 IL-11, MIP-1α (CCL3), MCP-1 (CCL2), MCP-2 (CCL8), GROγ (CXCL3), HGF, G-CSF and GM-CSF (Supplementary Table S1), and resembled largely those that are

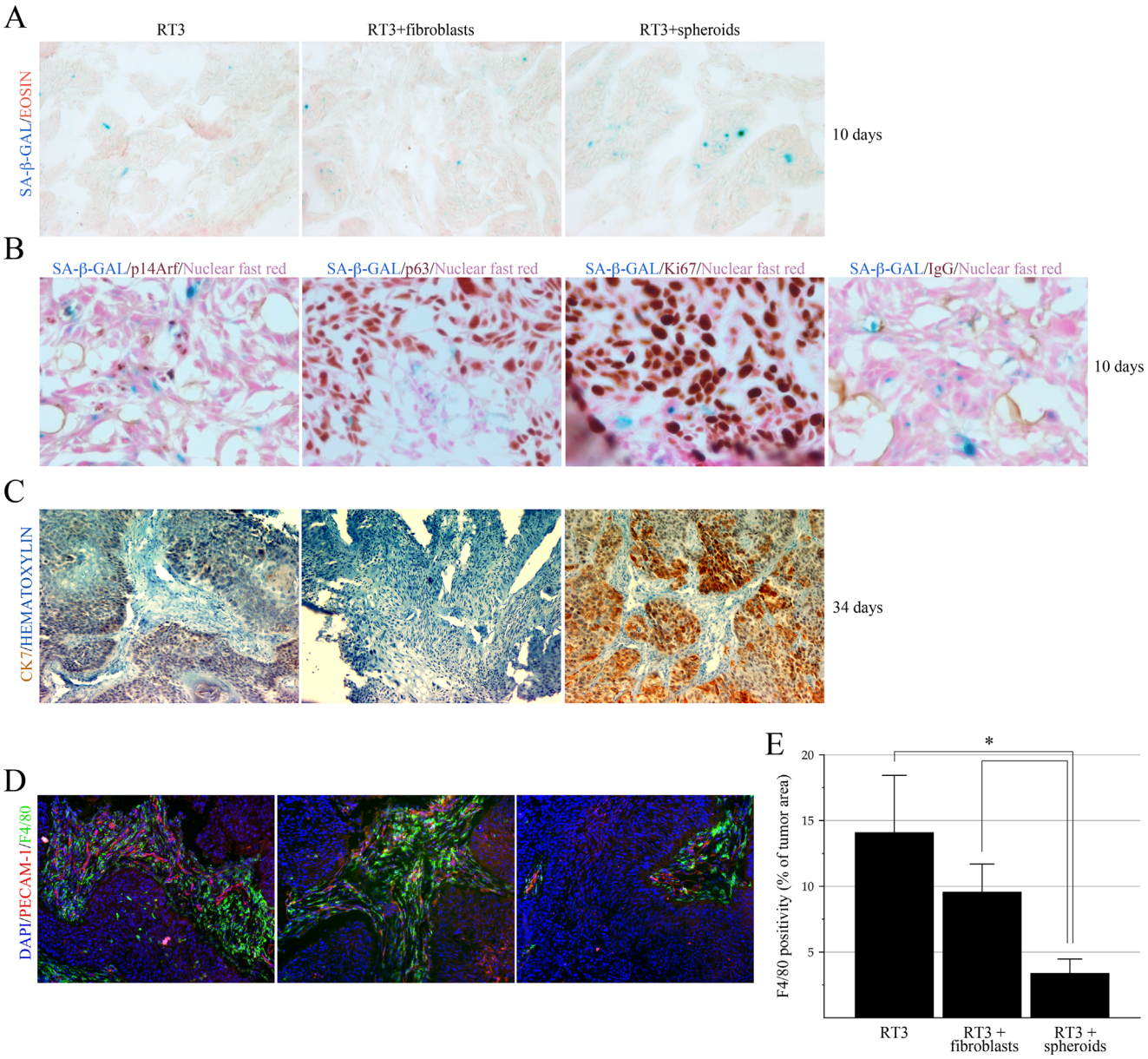

Fig. 5. Senescence-like phenotype observed *in vivo*. (A) SA-β-gal (blue) staining of tumors showed increased senescence in 10 days old RT3 tumors containing fibroblast spheroids compared to the RT3 cells implanted alone or with monolayer fibroblasts. Eosin (pink) was used as a counterstain. (B) Staining of p14Arf (brown), p63 (brown) and Ki67 in SA-β-gal (blue) positive areas in fibroblast spheroid-containing tumors at day 10 after tumor implantation. Nuclear fast red (pink) was used as a counterstain. IgG staining was used as a negative control (the panel on the right). (C) Increased CK7 (brown) mediated differentiation in fibroblast spheroid-containing RT3 tumors compared to tumors derived from RT3 cells alone or RT3 cell implanted with monolayer fibroblasts. Hematoxylin (blue) was used as a counterstain. (D) Decreased staining of macrophage marker F4/80 (green) in fibroblast spheroid containing RT3 tumors compared to tumor derived from RT3 cells alone or RT3 cell implanted with monolayer fibroblasts. DAPI (blue) and PECAM-1 (red) were used to show localization of cell nuclei and blood vessels, respectively. (E) Quantification of F4/80 positivity compared to tumor area.

induced during a senescence-associated secretory phenotype (SASP) [19] suggesting that this response is intended for paracrine signaling. Other important mediators of senescence, such as C/EBPβ (3.1 fold), GROα (5.8 fold) and KGF (3.5 fold), were also induced in nemotic fibroblasts according to microarray expression analysis.

To test whether the SASP-like phenotype of fibroblast spheroids was associated with senescence, we analyzed the expression of different senescence markers in fibroblast spheroids. Spheroids stained positive for SA-β-gal, the most widely used senescence marker, starting at 24 h with increasing intensity with time (Fig. 3(A)). Uniform SA-β-gal staining in frozen sections of spheroids excluded the possibility that SA-β-gal positivity was due to hypoxia or limited nutrient conditions in the center of the spheroid (data not shown). In addition, fibroblast spheroids showed gradual increase of the autofluorescence (Fig. 3(A)), a known phenomenon in senescent and ageing fibroblasts [20]. Surprisingly, the p53-p21 and Rb pathways, classical regulators of cellular senescence, were down-regulated in spheroids at the protein (Fig. 3(B)), and p53 also at the mRNA level (3.4-fold in microarray). Together with the observed up-regulation of p27, down-regulation of cyclin D1 (Fig. 2(D)), and the cell cycle arrest in G1/G0 phase, our results support a quiescent phenotype rather than senescence [18]. Since quiescence is a reversible cell cycle arrest, we studied the reversibility of the nemotic phenotype. Cells were first grown for 96 h as spheroids to induce cell cycle arrest and then transferred to a monolayer culture for the indicated times. In the monolayer culture cells resumed proliferation as judged by PCNA expression

indicating that nemosis is a reversible phenomenon (Fig. 3(C)). The reversibility of nemosis was further strengthened by the reversibility of SASP (shown by COX-2 expression), restoration of actin expression, and disappearance of the SA-β-gal positivity in response to the change in growth conditions (Fig. 3(C) and (D)).

To test whether malignant cells of fibroblast origin enter nemosis and arrest cell cycle, we studied two fibrosarcoma cell lines (HT-1080 and A9733). Both cell lines formed spheroids, but cells did not adhere as strongly to each other as normal fibroblasts (Fig. 4(A)). As anticipated, fibrosarcoma cells retained their ability to proliferate in spheroids, as judged by increased spheroid size (Fig. 4(A)), and sustained PCNA levels (Fig. 4(B)). Furthermore, actin levels were not down regulated in fibrosarcoma spheroids (Fig. 4(B)).

3.3. Nemotic fibroblasts induce senescence-like phenotype in tumors

The nemotic fibroblast spheroids secreted SASP-like molecules and these molecules are known to be able to modulate the behavior and growth of tumors [19,21]. To determine if reduced tumor growth in fibroblast spheroid-containing tumors was associated with induction of senescence in the tumor cells, we analyzed tumors grown only for 10 days, a time point after which the difference in the tumor growth between the groups started to appear (Fig. 1(C)). Interestingly, at this time point the fibroblast spheroid-containing tumors displayed marginally more SA-β-gal positive cells (Fig. 5(A)) and senescence-associated heterochromatin foci (SAHF) (Supplementary Fig. S3A) Tumor areas harboring SA-β-gal in fibroblast spheroid-containing tumors were also positive for p14Arf and negative for p63 and Ki67, suggesting the senescence like phenotype in the spheroid-containing tumors (Fig. 5(B)). Expression of p63 was slightly decreased also in entire spheroid-containing RT3 tumors compared to tumors derived from RT3 cells only or RT3 tumors containing monolayer fibroblasts (Supplementary Fig. S3B). At day 34 only 1/4 spheroid-containing tumor samples showed increased SA-β-gal positivity (Figure S3C), suggesting that fibroblast spheroids lost their activity over time. This was also supported by the observed induction of tumor growth at day 24 (Fig. 1(C)). However, increased cytokeratin-7 (CK7) -mediated differentiation of RT3 cells was detected at day 34 in the spheroid-containing RT3 tumors compared to RT3 alone or RT3 tumors containing monolayer fibroblasts (Fig. 5(C)). This is in line with an earlier observation that tumor cell senescence causes CK7-mediated differentiation [22]. The spheroid-containing tumors also showed significantly decreased macrophage infiltration as compared to the tumors formed from RT3 cells alone or from RT3 cells together with monolayer fibroblasts, indicating a difference in the immune response between the different groups (Fig. 5(D) and (E)). More detailed experiment is needed to elucidate the mechanism of decreased growth and senescence of fibroblast spheroid containing tumors.

4. Discussion

Fibroblasts seeded on a non-adhesive substrate form 3D multicellular spheroids and fibronectin-integrin connection has been shown to mediate this time-dependent clustering [23]. A major finding in the present study is that these nemotic fibroblasts inhibited the growth of tumor cells both *in vitro* and *in vivo* while the same fibroblasts grown on conventional 2D culture promoted the tumor growth. Importantly, in this regard the nemotic fibroblasts resembled the normal fibroblasts which have been shown to restrict tumor growth [2,3]. Mechanistically, fibroblast spheroids appeared to cause cellular senescence in adjacent cells in xenografts tumor cells. The nemosis-associated secretory phenotype identified in the gene expression analysis resembled largely that seen in senescence and included various cytokines and growth factors. This is agreement with earlier observations showing that SASP factors reinforce and cause senescence in adjacent cells, although it has been shown to cause proliferation arrest mainly in normal and premalignant cells and promote proliferation of malignant cells [19,21]. Notably, RT3 tumor had slight increase in senescence-like phenotype in response to nemotic fibroblast spheroids, although they harbor inactive p53 due to mutation [16]. Instead of p53, RT3 senescence was associated with upregulation of p14Arf, which is able to mediate senescence in p53-independent mechanism [24], and loss of p63, which is required for the p14Arf-mediated senescence [25].

Whether SASP causes an increase or decrease in adjacent cell proliferation or even senescence might be dependent on additional environmental stress factors [21]. Although, the nemotic fibroblasts appeared to function in a similar way as SASP, secretory phenotype associated to nemotic fibroblasts may still have crucial differences to SASP that limit their tumor promoting capabilities. We have earlier shown in 2D *in vitro* studies that conditioned medium from fibroblast spheroids causes increased proliferation of RT3 cells and that it is associated with increased expression of p63 [15], whereas here we detected that nemotic fibroblasts decreased RT3 colonies in soft-agar and inhibited tumor growth in mice, which was associated with decreased expression of p63, suggesting that RT3 cells respond differently to nemosis in 3D than in 2D.

In addition to senescence, fibroblast spheroids caused differentiation of RT3 tumors, as measured by CK7 expression. This is in accordance with previous finding that conditioned medium from the fibroblast spheroids can cause differentiation and growth arrest of leukemia and myeloma cells [12,26]. Interestingly, restoration of senescence in liver tumors results in CK7-mediated differentiation [22], and furthermore, CK7-mediated cell differentiation was found to be adjacent to senescent hepatocytes [27], suggesting a close interplay between CK7 and senescence. This suggests that the secretory phenotype of fibroblast spheroids, which resembles SASP, could promote CK7-mediated differentiation. However, additional experimentation is needed to clarify the exact mechanism how fibroblast spheroids prevent tumor growth.

Although the fibroblast phenotype in spheroids shares features of senescence, such as secretory phenotype and SA-β-gal positivity, it resembled more quiescence. Most importantly, nemosis was shown to be reversible; cells were able to resume cell cycle and lost secretory phenotype. Senescence is always irreversible phenotype, whereas cells in quiescence are able to resume cell cycle when growth conditions change [28,29]. Moreover, reversibility of secretory phenotype is in agreement with a recent report showing that quiescent fibroblasts are more active in mounting robust inflammatory responses than proliferative fibroblasts, especially in regards of COX2 expression [30]. Furthermore, they lacked induction of known senescence pathways. In senescence, cell cycle arrest is maintained by up-regulation of cell cycle inhibitors, such as p14Arf, p16, p21, p53 and Rb. Simultaneously cyclins D and E that drive the cell cycle, are expressed at high levels [31]. In contrast, in nemosis a universal down-regulation of cell cycle associated genes such as cyclins and cell cycle inhibitors (p53-p21 and Rb) occurred, suggesting a quiescence rather than senescence mode of cell cycle arrest. Even though SA-β-gal staining is a widely used marker of cellular senescence, SA-β-gal is also expressed in contact-inhibited fibroblasts [17]. Hence, although nemotic fibroblasts share many common features with cellular senescence it is a novel phenotype that has not been previously described.

Nemotic activation has not yet been identified *in vivo*, but one can speculate that situations where fibroblasts lose their contact to connective tissue it might happen. In inflammation, cancer and

wound healing, different proteases destroys connective tissue that could lead to a liberation of fibroblasts from ECM and direct them to cluster together. This is supported by the finding that activated myofibroblasts are known to make direct cell-cell contacts, adherens and gap junctions, during wound healing *in vivo* [32]. Furthermore, CAF's are know to secrete similar mediators of inflammation as nemotic fibroblasts, such as IL-1α, IL-1β, IL-6, HGF, plasminogen activators and COX-2 [1]. Taken together, although there is no direct evidence that nemotic fibroblasts are found in tumors vast amount of data exist suggesting that nemotic fibroblasts poses similar properties as stromal fibroblasts.

Taken together we show that when fibroblasts lost their adhesion to a solid surface and clustered they reacted to the altered growth conditions by arresting their cell cycle and secreting paracrine molecules into their microenvironment. We suggest that with respect to tumor biology nemotic fibroblasts would resemble the normal, sustained quiescent fibroblasts and their function *in vivo* should in future be studied in other tumor models.

Competing interests

None.

Acknowledgements

The authors declare that they have no competing financial interests. We thank Irina Suomalainen and Selina Mäkinen for expert technical assistance, Drs. Esko Kankuri and Jozef Bizik for help with microarray and Dr. Petteri Arstila for advice in FACS analysis. This work was supported by grants from the Magnus Ehrnrooth Foundation, the Finnish Medical Foundation, Academy of Finland, Finnish Cancer Organizations, and the European Community's 7th Framework Programme FP7/2007-2011 under grant agreement no. 201279 (PL). PS and P-RK have been supported by the Helsinki Graduate Program in Biotechnology and Molecular Biology.

Appendix A. Supplementary material

Supplementary data associated with this article can be found in the online version at http://dx.doi.org/10.1016/j.yexcr.2016.05.005.

References

[1] K. Räsänen, A. Vaheri, Activation of fibroblasts in cancer stroma, Exp. Cell Res. 316 (2010) 2713–2722.
[2] R. Kalluri, M. Zeisberg, Fibroblasts in cancer, Nat. Rev. Cancer 6 (2006) 392–401.
[3] M.J. Bissell, W.C. Hines, Why don't we get more cancer? A proposed role of the microenvironment in restraining cancer progression, Nat. Med. 17 (2011) 320–329.
[4] H.A. Coller, L. Sang, J.M. Roberts, A new description of cellular quiescence, PLoS Biol. 4 (2006) e83.
[5] J.M. Lemons, X.J. Feng, B.D. Bennett, A. Legesse-Miller, E.L. Johnson, I. Raitman, E.A. Pollina, H.A. Rabitz, J.D. Rabinowitz, H.A. Coller, Quiescent fibroblasts exhibit high metabolic activity, PLoS Biol. 8 (2010) e1000514.
[6] A. Vaheri, A. Enzerink, K. Räsänen, P. Salmenperä, Nemosis, a novel way of fibroblast activation, in inflammation and cancer, Exp. Cell Res. 315 (2009) 1633–1638.
[7] J. Bizik, E. Kankuri, A. Ristimäki, A. Taieb, H. Vapaatalo, W. Lubitz, A. Vaheri, Cell-cell contacts trigger programmed necrosis and induce cyclooxygenase-2 expression, Cell Death Differ. 11 (2004) 183–195.
[8] A. Greenhough, H.J. Smartt, A.E. Moore, H.R. Roberts, A.C. Williams, C. Paraskeva, A. Kaidi, The COX-2/PGE2 pathway: key roles in the hallmarks of cancer and adaptation to the tumour microenvironment, Carcinogenesis 30 (2009) 377–386.
[9] K. Räsänen, I. Virtanen, P. Salmenperä, R. Grenman, A. Vaheri, Differences in the nemosis response of normal and cancer-associated fibroblasts from patients with oral squamous cell carcinoma, PLoS One 4 (2009) e6879.
[10] E. Kankuri, D. Cholujova, M. Comajova, A. Vaheri, J. Bizik, Induction of hepatocyte growth factor/scatter factor by fibroblast clustering directly promotes tumor cell invasiveness, Cancer Res. 65 (2005) 9914–9922.
[11] V. Sirén, P. Salmenperä, E. Kankuri, J. Bizik, T. Sorsa, T. Tervahartiala, A. Vaheri, Cell-cell contact activation of fibroblasts increases the expression of matrix metalloproteinases, Ann. Med. 38 (2006) 212–220.
[12] E. Kankuri, O. Babusikova, K. Hlubinova, P. Salmenperä, C. Boccaccio, W. Lubitz, A. Harjula, J. Bizik, Fibroblast nemosis arrests growth and induces differentiation of human leukemia cells, Int. J. Cancer 122 (2008) 1243–1252.
[13] A. Enzerink, P. Salmenperä, E. Kankuri, A. Vaheri, Clustering of fibroblasts induces proinflammatory chemokine secretion promoting leukocyte migration, Mol. Immunol. 46 (2009) 1787–1795.
[14] K. Räsänen, P. Salmenperä, M. Baumann, I. Virtanen, A. Vaheri, Nemosis of fibroblasts is inhibited by benign HaCaT keratinocytes but promoted by malignant HaCaT cells, Mol. Oncol. 2 (2008) 340–348.
[15] K. Räsänen, A. Vaheri, Proliferation and motility of HaCaT keratinocyte derivatives is enhanced by fibroblast nemosis, Exp. Cell Res. 316 (2010) 1739–1747.
[16] N.E. Fusenig, P. Boukamp, Multiple stages and genetic alterations in immortalization, malignant transformation, and tumor progression of human skin keratinocytes, Mol. Carcinog. 23 (1998) 144–158.
[17] G.P. Dimri, X. Lee, G. Basile, M. Acosta, G. Scott, C. Roskelley, E.E. Medrano, M. Linskens, I. Rubelj, O. Pereira-Smith, A biomarker that identifies senescent human cells in culture and in aging skin *in vivo*, Proc. Natl. Acad. Sci. USA 92 (1995) 9363–9367.
[18] V.A. Blomen, J. Boonstra, Cell fate determination during G1 phase progression, Cell Mol. Life Sci. 64 (2007) 3084–3104.
[19] J.P. Coppe, P.Y. Desprez, A. Krtolica, J. Campisi, The senescence-associated secretory phenotype: the dark side of tumor suppression, Annu. Rev. Pathol. 5 (2010) 99–118.
[20] T. von Zglinicki, E. Nilsson, W.D. Docke, U.T. Brunk, Lipofuscin accumulation and ageing of fibroblasts, Gerontology 41 (Suppl. 2) (1995) 95–108.
[21] T. Kuilman, D.S. Peeper, Senescence-messaging secretome: SMS-ing cellular stress, Nat. Rev. Cancer 9 (2009) 81–94.
[22] W. Xue, L. Zender, C. Miething, R.A. Dickins, E. Hernando, V. Krizhanovsky, C. Cordon-Cardo, S.W. Lowe, Senescence and tumour clearance is triggered by p53 restoration in murine liver carcinomas, Nature 445 (2007) 656–660.
[23] P. Salmenperä, E. Kankuri, J. Bizik, V. Siren, I. Virtanen, S. Takahashi, M. Leiss, R. Fassler, A. Vaheri, Formation and activation of fibroblast spheroids depend on fibronectin-integrin interaction, Exp. Cell Res. 314 (2008) 3444–3452.
[24] L. Ha, T. Ichikawa, M. Anver, R. Dickins, S. Lowe, N.E. Sharpless, P. Krimpenfort, R.A. Depinho, D.C. Bennett, E.V. Sviderskaya, G. Merlino, ARF functions as a melanoma tumor suppressor by inducing p53-independent senescence, Proc. Natl. Acad. Sci. USA 104 (2007) 10968–10973.
[25] L. Ha, R.M. Ponnamperuma, S. Jay, M.S. Ricci, W.C. Weinberg, Dysregulated DeltaNp63alpha inhibits expression of Ink4a/arf, blocks senescence, and promotes malignant conversion of keratinocytes, PLoS One 6 (2011) e21877.
[26] K. Szabova, I. Bizikova, M. Mistrik, J. Bizik, Inflammatory environment created by fibroblast aggregates induces growth arrest and phenotypic shift of human myeloma cells, Neoplasma 62 (2015) 938–948.
[27] H. Ikeda, M. Sasaki, Y. Sato, K. Harada, Y. Zen, T. Mitsui, Y. Nakanuma, Bile ductular cell reaction with senescent hepatocytes in chronic viral hepatitis is lost during hepatocarcinogenesis, Pathol. Int. 59 (2009) 471–478.
[28] J. Campisi, F. d'Adda di Fagagna, Cellular senescence: when bad things happen to good cells, Nat. Rev. Mol. Cell Biol. 8 (2007) 729–740.
[29] H.A. Coller, Cell biology. The essence of quiescence, Science 334 (2011) 1074–1075.
[30] B.R. Chen, H.H. Cheng, W.C. Lin, K.H. Wang, J.Y. Liou, P.F. Chen, K.K. Wu, Quiescent fibroblasts are more active in mounting robust inflammatory responses than proliferative fibroblasts, PLoS One 7 (2012) e49232.
[31] M.V. Blagosklonny, Cell cycle arrest is not senescence, Aging 3 (2011) 94–101.
[32] H.P. Ehrlich, T. Diez, Role for gap junctional intercellular communications in wound repair, Wound Repair Regen. 11 (2003) 481–489.